

Improvement on the manipulation of a single nitrogen-vacancy spin and microwave photon at single-quantum level

Yuan Zhou^{1,*}, Dong-Yan Lü¹, Guang-Hui Wang², Yan-Hua Fu¹,
Ming-Yao He¹ and Hong-Tao Ren³

¹ School of Science, Hubei University of Automotive Technology, Shiyan 442002, China

² Department of of Automobile Engineering, Hubei University of Automotive Technology, Shiyan 442002, China

³ School of Materials Science and Engineering, Liaocheng University, Liaocheng 252000, China

E-mail: zhouyuan@huat.edu.cn

Received 17 January 2021, revised 5 March 2021

Accepted for publication 5 March 2021

Published 9 April 2021



Abstract

It remains a great challenge to realize direct manipulation of a nitrogen-vacancy (NV) spin at the single-quantum level with a microwave (MW) cavity. As an alternative, a hybrid system with the spin–phonon–photon triple interactions mediated by a squeezed cantilever-type harmonic resonator is proposed. According to the general mechanical parametric amplification of this in-between phonon mode, the direct spin–phonon and photon–phonon couplings are both exponentially enhanced, which can even further improve the coherent manipulation of a single NV spin and MW photon with a higher efficiency. In view of this triple system with enhanced couplings and the additional sideband adjustable designs, this scheme may provide a more efficient phonon-mediated platform to bridge or manipulate the MW quantum and a single electron spin coherently. It is also hoped to evoke wider applications in the areas of quantum state transfer and preparation, ultrasensitive detection and quantum nondestructive measurement, etc.

Keywords: NV center, mechanical parametric amplification, quantum manipulation

(Some figures may appear in colour only in the online journal)

1. Introduction

Implementing quantum manipulations and quantum simulations in the microwave (MW) domain has stimulated huge progress in recent times [1–3]. Designing a hybrid quantum system in this special electromagnetic frequency region and implementing efficient quantum information processing (QIP) is gradually becoming recognized as one of the most reliable technological routes [4–7], whereupon the most central task lies in the achievement of perfect manipulation of atoms or artificial atoms utilizing these kinds of MW quantum devices [8], i.e. the MW cavity [9, 10], the MW waveguide [11, 12], the superconductive circuit [13, 14], etc. In addition, it is also regarded as a promising attempt to perform well-controlled quantum measurement or

quantum sensing with ultrasensitivity [15, 16] through fabricating MW-based hybrid setups or devices [17]. With the rapid development of high-quality MW devices integrating technology, the prospect of using MW to dominate QIP is also becoming clearer [18, 19].

Regarding today's mainstream schemes on QIP, and comparing all kinds of quantum units applicable for manipulation, the nitrogen-vacancy (NV) center in diamond is particularly attractive due to its excellent spin properties, i.e. ultrasensitivity to magnetic fields, fast MW manipulation, optical preparation and detection, and long coherence time even at ambient conditions [20–23]. The long spin coherence of NVs can also evoke many intriguing applications at the single-photon as well as macroscopic level. For example, it is a high-quality MW emitter in a diamond maser scheme proposed by Jin *et al* [24], which was also experimentally

* Author to whom any correspondence should be addressed.

demonstrated by Breeze group in 2018 [25], etc. However, due to the inherent limitation of magnetic coupling mechanism and magnetic field localization degree, it remains a considerable huge challenge to realize a direct strong magnetic coupling to single NV spin in a given MW device [26, 27], especially in the MW cavity [28].

In a different way, here we discuss a different approach and propose a hybrid system with phonon-mediated spin–phonon–photon triple interactions, in which a squeezed quantum mechanical mode can not only interact with an NV spin through the first-order gradient magnetic field, but also capacitively couple to the MW cavity [29–32]. Utilizing the general mechanical parametric amplification (MPA), we can significantly enhance two pairs of direct spin–phonon and photon–phonon couplings both with the exponential rate ($\sim e^r$) in a new squeezed frame [29, 33–38]. For a given squeezing parameter r , we can further adjust both coupled pairs to obey the Jaynes–Cummings (JC)-type or anti-Jaynes–Cummings-type interactions, only through modulating the parameters $\Delta_{c/q}$. We state both $\Delta_{c/q}$ are conveniently tunable parameters with respect to the processes of MW cavity linearization and dressed-state NVs. In view of this hybrid quantum system with adjustable sidebands and enhanced couplings, our scheme may provide a more efficient phonon-mediated quantum interface to bridge the MW quanta and a single electron spin coherently, and even provide a fruitful route towards the manipulation of a single NV spin and MW photon at the single-quantum level with an improved efficiency. We also hope this result may evoke wider applications in the areas of quantum state transfer [39, 40], ultrasensitive detection [41], quantum nondestructive measurement (QND) [42], etc.

2. Setup

The whole schematic design and relevant physical image are all illustrated in figures 1(a)–(c). Working as a mediator, a cantilever-type mechanical resonator (MR) interacts with the MW cavity and a single NV spin, and its spring constant is also periodically tunable, so we can obtain the second-order nonlinear interaction on this mechanical mode [29, 38, 43–45]. In a new squeezed frame, the quantum fluctuation of this MR amplitude is amplified exponentially with $\sim e^r$, known as the MPA [29]. As specified in figure 1(a), there are two essential direct strong-coupling parts to form this triple photon–phonon–spin interaction system. For the first part, a sharp nanomagnetic tip is attached at the end of the cantilever with a designed tunable spring constant, just above which a single NV center is set near to this nanomagnet; we can then obtain the strong magnetic spin–phonon coupling with the dressed-state expression $\sim \lambda e^r (\hat{b} + \hat{b}^\dagger)(\hat{\sigma}^+ + \hat{\sigma}^-)$ in a squeezed frame [29]. We also state another available strain phonon coupling setup, i.e. the investigations [46–50]. For the second part, we can also perform the strong coupling through the capacitive interaction between the MW cavity and the MR [32, 51]. As shown in figure 1(a), a superconducting coplanar cavity is connected to the MR through the capacitor circuit.

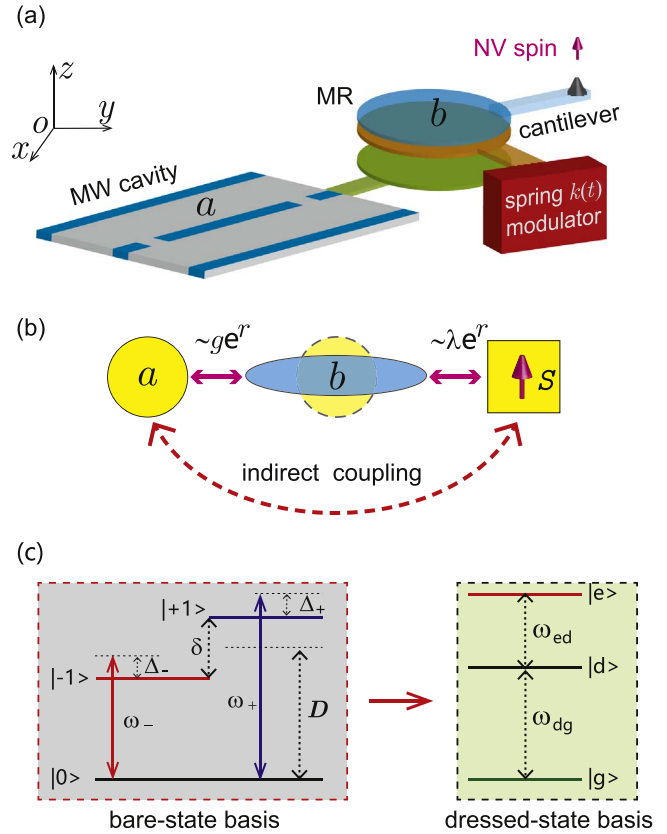


Figure 1. (Color online) (a) Potential photon–phonon–spin hybrid setup with respect to the triple coupling system mediated by a squeezed mechanical mode. A sharp nano magnetic tip is attached at the end of the silicon cantilever with its tunable spring constant, above which a single NV center is set near to this magnet. A superconducting coplanar MW cavity also couples to this mechanical cantilever through capacitive interactions. As a result, it is available for this MR to achieve capacitive coupling to the MW cavity and magnetic coupling to the single NV spin, respectively. (b) Schematic of enhancing the indirect coupling between the MW cavity and single NV spin through MPA. (c) Ground-state energy diagram for a single NV center in the basis of bare state and dressed state.

Then, we can obtain the so-called cavity optomechanical coupling system, and acquire an exponentially enhanced interaction as $\sim ge^r (\hat{b} + \hat{b}^\dagger)(\hat{a} + \hat{a}^\dagger)$, after the cavity mode is linearized [32, 51].

3. Mechanism of this triple coupling system

As illustrated in figure 1(a), we assume that the spring constant of this mechanical cantilever is a periodically tunable parameter with the frequency ω_χ . According to the statement in the detail of appendix A, we can obtain the Hamiltonian of this quantized cantilever with the second-order nonlinear interaction

$$\hat{H}_{mr} \simeq \omega_m \hat{b}^\dagger \hat{b} - \frac{\Omega_\chi}{2} (\hat{b}^{\dagger 2} e^{2i\omega_\chi t} + \hat{b}^2 e^{2i\omega_\chi t} + \text{h.c.}). \quad (1)$$

In equation (1), we have discarded the energy-shift item caused by this nonlinear drive amplitude Ω_χ .

According to figure 1(c), for the first NV–MR coupling pair, we apply the dichromatic MW fields to dress the ground state of the NV center, and acquire the efficient spin–phonon transition channel according to appendix B. In a selected dressed-state subspace $\{|d\rangle, |g\rangle\}$, the effective spin–phonon interaction can be rewritten as the JC-type Hamiltonian

$$\hat{H}_{\text{sp}}^d \simeq \frac{\omega_0}{2} \hat{\sigma}_z + \lambda(\hat{b}^\dagger \hat{\sigma}^- + \hat{b} \hat{\sigma}^+). \quad (2)$$

Here, we define $\omega_0 \equiv \omega_{dg}$, $\hat{\sigma}_z \equiv \hat{\sigma}_{dd} - \hat{\sigma}_{gg}$, and $\hat{\sigma}^\pm \equiv \hat{\sigma}_{dg}^\pm$ for simplicity.

For another pair of MR–cavity coupling, we assume the MW cavity interacts with the MR capacitively, which forms the so-called cavity optomechanical coupling pair. This type of interaction is described as

$$\begin{aligned} \hat{H}_{\text{op}} &\simeq [\omega_c + g_0(\hat{b}^\dagger + \hat{b})] \hat{a}^\dagger \hat{a} \\ &+ \beta(\hat{a}^\dagger e^{i\omega_L t} + \text{h.c.}). \end{aligned} \quad (3)$$

In equation (3), the first two items describe the general optomechanical coupling with the fundamental cavity frequency ω_c and the optomechanical coupling strength g_0 , and the last item means the classical MW laser drive to this cavity mode with driving amplitude β and frequency ω_L . Utilizing the standard linearization method with $\hat{a} = \alpha + \delta\hat{a}$ and $\hat{a}^\dagger = \alpha^* + \delta\hat{a}^\dagger$ [32, 51], we can linearize this optomechanical interaction (3) as

$$\hat{H}_{\text{op}}^L \simeq \delta_c \hat{a}^\dagger \hat{a} + g(\hat{a}^\dagger \hat{b} + \hat{a} \hat{b}^\dagger), \quad (4)$$

in which the parameters are assumed as $\delta_c = \omega_c - \omega_L$, $\alpha^* = \alpha$, and $g = g_0\alpha$, and we have set $\delta\hat{a}^{(\dagger)} \equiv \hat{a}^{(\dagger)}$ for simplicity.

As a result, together with equations (1), (2), and (4), we can obtain the whole Hamiltonian for describing this phonon-mediated three-body hybrid system:

$$\hat{H}_w = \hat{H}_{\text{mr}} + \hat{H}_{\text{op}}^L + \hat{H}_{\text{sp}}^d. \quad (5)$$

Then, we apply an unitary transformation $\hat{U}_0 = \exp[i\hat{H}_0 t]$ to equation (5) with $\hat{H}_0 = \omega_\chi(\hat{b}^\dagger \hat{b} + \hat{a}^\dagger \hat{a} + \hat{\sigma}_z/2)$. In this new rotating frame, we can obtain

$$\begin{aligned} \hat{H}_w' &\simeq \delta_m \hat{b}^\dagger \hat{b} - \frac{\Omega_\chi}{2}(\hat{b}^{\dagger 2} + \hat{b}^2) + \Delta_c \hat{a}^\dagger \hat{a} + \frac{\Delta_q}{2} \hat{\sigma}_z \\ &+ g(\hat{a}^\dagger \hat{b} + \hat{a} \hat{b}^\dagger) + \lambda(\hat{b}^\dagger \hat{\sigma}^- + \hat{b} \hat{\sigma}^+), \end{aligned} \quad (6)$$

with $\delta_m = \omega_m - \omega_\chi$, $\Delta_c = \delta_c - \omega_\chi$, and $\Delta_q = \omega_0 - \omega_\chi$.

Considering this Hamiltonian (6) accompanied by the second-order nonlinear interaction of this mechanical freedom, we can utilize the standard unitary transformation $\hat{U}_s(r) = \exp[r(\hat{b}^2 - \hat{b}^{\dagger 2})/2]$ to diagonalize this mechanical mode belonging to \hat{H}_w' , where the squeezing parameter r is defined by $\tanh 2r = \Omega_\chi/\delta_m$. In this squeezed frame, we can obtain the Hamiltonian with the new expression

$$\begin{aligned} \hat{H}_w^S &\simeq \Delta_m \hat{b}^\dagger \hat{b} + \Delta_c \hat{a}^\dagger \hat{a} + \frac{\Delta_q}{2} \hat{\sigma}_z \\ &+ ge^r(\hat{b} + \hat{b}^\dagger)(\hat{a} + \hat{a}^\dagger) + \lambda e^r(\hat{b} + \hat{b}^\dagger) \hat{\sigma}_x, \end{aligned} \quad (7)$$

with $\Delta_m = \delta_m/\cosh 2r$. Here, it is noted that we have omitted the weak disturbance items during this

diagonalization process, because of their diminishing coefficients ($\propto e^{-r}$) as we increase the squeezing parameter r . In the interaction picture (IP), we obtain

$$\begin{aligned} \hat{H}_{\text{IP}}^S(t) &\approx G_1(\hat{b}\hat{a}e^{-i\delta_1 t} + \hat{b}^\dagger \hat{a}e^{-i\delta_2 t} + \text{h.c.}) \\ &+ G_2(\hat{b}\hat{\sigma}^-e^{-i\delta_3 t} + \hat{b}^\dagger \hat{\sigma}^-e^{-i\delta_4 t} + \text{h.c.}), \end{aligned} \quad (8)$$

with $G_1 = ge^r$, $G_2 = \lambda e^r$, $\delta_1 = \Delta_c + \Delta_m$, $\delta_2 = \Delta_c - \Delta_m$, $\delta_3 = \Delta_q + \Delta_m$, and $\delta_4 = \Delta_q - \Delta_m$. For a realistic condition, the dynamical evolution of this hybrid system is dominated by the master equation effectively as follows:

$$\begin{aligned} \frac{d\hat{\rho}}{dt} &= i[\hat{\rho}, \hat{H}_w^S(\hat{H}_{\text{IP}}^S)] + \kappa_1 \mathcal{D}[\hat{a}]\hat{\rho} \\ &+ \kappa_{\text{eff}}^S \mathcal{D}[\hat{b}]\hat{\rho} + \gamma \mathcal{D}[\hat{\sigma}_z]\hat{\rho}, \end{aligned} \quad (9)$$

where $\mathcal{D}[\hat{o}]\hat{\rho} = \hat{o}\hat{\rho}\hat{o}^\dagger - \hat{\rho}\hat{o}^\dagger\hat{o}/2 - \hat{o}^\dagger\hat{o}\hat{\rho}/2$, $\hat{\rho}$ is the density matrix of this three-body quantum system, and κ_1 , κ_{eff}^S , and γ correspond to the MW cavity dissipation rate, the effective squeezed MR damping rate, and the NV dephasing rate, respectively.

In this squeezed frame, the mechanical mode is fast and strongly damped with a large effective dissipation rate κ_{eff}^S [38, 52]. In this case, we can inevitably maintain this phonon mode in its ground state $|0\rangle$ and neglect the populations of any excited modes. This squeezed mechanical mode is then considered as an artificial or engineered reservoir of the heat phonon. In contrast, we can also apply an auxiliary cooling system or design to suppress its effective dissipation rate at the same magnitude as $\sim \kappa_1$, according to investigations [52–56].

Considering Hamiltonian (8), we also note, for a given cantilever with a certain squeezing parameter r , that Δ_m is very small and untunable. However, Δ_c and Δ_q are both tunable parameters, which can be implemented via the cavity-resonator linearization process and NV-resonator MW dressed process. Through modulating both relevant parameters, we can obtain an effective triple Hamiltonian with distinct expressions. Utilizing this, we can also carry out different simulations for multiple applications. For example, in case (i), when $\Delta_c - \Delta_m \simeq \Delta_q - \Delta_m \simeq 0$, the Hamiltonian reduces to the beam-split-type interaction effectively, with $\sim \hat{b}^\dagger [G_1 \hat{a} + G_2 \hat{\sigma}^-] + \text{h.c.}$, which is applicable for establishing a quantum interface to bridge the MW photons and NV spin efficiently. In case (ii), when $\Delta_c + \Delta_m \simeq \Delta_q - \Delta_m \simeq 0$ (or $\Delta_c - \Delta_m \simeq \Delta_q + \Delta_m \simeq 0$), the Hamiltonian reduces to the types of $\sim \hat{b}^\dagger [G_1 \hat{a}^\dagger + G_2 \hat{\sigma}^-] + \text{h.c.}$ (or $\sim \hat{b}^\dagger [G_1 \hat{a} + G_2 \hat{\sigma}^+] + \text{h.c.}$), which is suitable for engineering the MW photons and NV spin into the nonclassical steady states, such as certain entanglement or quantum correlation. In case (iii), once $\Delta_c + \Delta_m \simeq \Delta_q + \Delta_m \simeq 0$, the Hamiltonian is also reduced to the form $\sim \hat{b}^\dagger [G_1 \hat{a}^\dagger + G_2 \hat{\sigma}^+] + \text{h.c.}$ effectively, which can also be applied to the preparation of special nonclassical states; i.e. governed by this type of interaction, an investigation on generating the Bell-type maximum entanglement through a fast dissipation process was recently reported [57]. Taking cases (i) and (ii) as examples, we present specific discussions

and numerical simulations of relevant applications in the following section.

4. Applications

4.1. Efficiency improvement on quantum state transfer between the NV spin and MW photon

For case (i), the effective Hamiltonian reduces to

$$\hat{H}_{(ii)}^S \simeq (G_1 \hat{b}^\dagger \hat{a} + G_2 \hat{b} \hat{\sigma}^+ + \text{h.c.}). \quad (10)$$

Utilizing this interaction, we can implement the target of quantum state transfer from the MW photons to an NV spin mediated by this squeezed phonon mode, and vice versa [39, 40]. Therefore, the first application of this scheme is focused on establishing a quantum spin–photon interface with further improved efficiency.

For an ideal condition without considering any decoherence factors, this triple-interaction system is governed by the Schrödinger equation $i\partial|\Psi(t)\rangle/\partial t = \hat{H}_{(ii)}^S|\Psi(t)\rangle$. Taking the quantum state transfer from the MW photon to NV spin at the single-quantum level as an example, we first assume this photon mode is reduced to the lowest subspace $\{|0\rangle, |1\rangle\}$ for simplicity. Without loss of generality, the initial state of the MW cavity is assumed as $|\psi\rangle_{\text{MW}} = \alpha|0\rangle + \beta|1\rangle$ with the normalizing condition $|\alpha|^2 + |\beta|^2 = 1$, and the mechanical mode and NV spin are both initialized in their ground states $|0\rangle_m$ and $|g\rangle_s$. Therefore, the initial state of this whole system is initialized in the assumed state $|\Psi(0)\rangle = |\psi\rangle_{\text{MW}} \otimes |0\rangle_m \otimes |g\rangle_s$, and the relevant quantum information to be transferred to NV spin is initially coded in the freedom of this MW mode with the given coefficients α and β .

Here we assume $g \simeq \lambda$ and $G_1 = -G_2 = G = ge^r$ for simplicity, and this whole system is dominated by Hamiltonian (10). Through solving this Schrödinger equation, we can obtain its evolved state $|\Psi(t)\rangle$ analytically at any arbitrary time t . At the special moment with $\tau_s \sim \pi/G = \pi/(ge^r)$, we can obtain the target state with $|\Psi(\tau_s)\rangle = |0\rangle_{\text{MW}} \otimes |0\rangle_m \otimes |\psi\rangle_s$ and $|\psi\rangle_s = \alpha|g\rangle + \beta|d\rangle$. Then, we can reach the target of transferring the arbitrary quantum information of MW mode to NV spin and vice versa. Furthermore, its transfer efficiency will be further improved significantly by this squeezed mechanical mode owing to the amplification of both coupling strength and rate e^r [29].

To indicate this physical process more clearly and intuitively, we need to carry out the relevant numerical simulation on it. Considering all adverse decoherence factors in our numerical simulation, its dynamical evolution is governed by the master equation $d\hat{\rho}/dt = i[\hat{\rho}, \hat{H}_{(ii)}^S] + \kappa_1 \mathcal{D}[\hat{a}]\hat{\rho} + \kappa_{\text{eff}}^S \mathcal{D}[\hat{b}]\hat{\rho} + \gamma \mathcal{D}[\hat{\sigma}_z]\hat{\rho}$. In general, here we set $\alpha = 0.6$, $\beta = 0.8$, $\kappa_1 \sim \gamma \sim 0.01g$, and $\kappa_{\text{eff}}^S \sim 0.1g$ for simplicity; then, we can solve this master equation numerically and achieve dynamical fidelity according to the definition $F = \langle \Psi(\tau_s) | \hat{\rho}(t) | \Psi(\tau_s) \rangle$, namely the overlap between the target state $|\Psi(\tau_s)\rangle$ and the dynamically evolved states $\hat{\rho}(t) = |\Psi(t)\rangle \langle \Psi(t)|$ at arbitrary moment t .

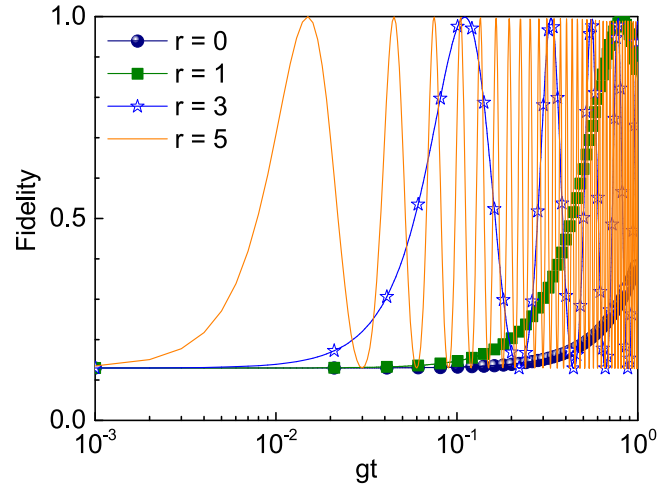


Figure 2. (Color online) Dynamical fidelity for this photon–spin state transfer process. The parameters are set as $g = \lambda$, $r = 0$ the black solid line with solid spheres, $r = 1$ the olive solid line with solid squares, $r = 3$ the blue solid line with open stars, and $r = 5$ the orange solid line, $\kappa_1 \sim \gamma \sim 0.01g$, and $\kappa_{\text{eff}}^S \sim 0.1g$.

The corresponding numerical results are plotted in figure 2, and these numerical results are highly consistent with our analysis above. We note that the fidelity can be near to 1 infinitely in the first few periods of oscillation in time, regardless of whether the squeezing parameter is set as $r = 1$, $r = 3$, or $r = 5$, and even with all of the decoherence factors being considered in this master equation. In addition, the relevant state-transfer efficiency and velocity can also be further improved significantly as we increase the squeezing parameter r from $r = 0$ to $r = 5$, and its shortest time interval for transfer satisfies $\tau_s \propto e^{-r}$.

4.2. Engineering NV spin and MW photon into the quantum correlated state indirectly by the squeezed phonon mode

In contrast, for case (ii), the effective Hamiltonian obeys the forms of

$$\hat{H}_{(ii)}^{S(1)} \simeq (G_1 \hat{b}^\dagger \hat{a}^\dagger + G_2 \hat{b} \hat{\sigma}^+ + \text{h.c.}), \quad (11)$$

or

$$\hat{H}_{(ii)}^{S(2)} \simeq (G_1 \hat{b}^\dagger \hat{a} + G_2 \hat{b} \hat{\sigma}^+ + \text{h.c.}). \quad (12)$$

Dominated by both types of triple interactions, we can also carry out the task of engineering the MW photon and NV spin into the steady nonclassical state, utilizing different routes such as the adiabatic evolution or fast dissipation, etc [38, 52, 57–60]. Taking Hamiltonian (11) as an example, we first assume G_1 is opposite to G_2 in phase and $G_1 \neq G_2$; then, we can rewrite this Hamiltonian as $\hat{H}_{(ii)}^{S(1)} \simeq \hat{b}(G_2 \hat{\sigma}^+ - G_1 \hat{a}) + \text{h.c.}$. We note this type of interaction is quite similar to the general Hamiltonian for engineering the two-mode quantum correlated state assisted by fast dissipation [60–63]. In this scheme, we stress that the photon–phonon and spin–phonon coupling can be exponentially enhanced in a squeezed frame; however, the

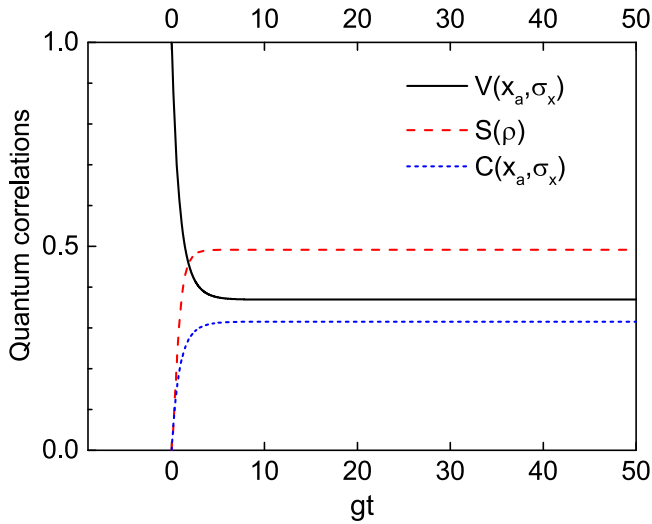


Figure 3. (Color online) Time-dependent quantum correlations of the MW photon and NV spin. The parameters are set as $\lambda = -0.7g$, $r = 2$, $\kappa_1 \sim \gamma \sim 0.01g$, and $\kappa_{\text{eff}}^S \sim 200g$, where the black solid line means the joint variance $V(\hat{X}_a, \hat{\sigma}_x)$, the red dashed line means the VNE $S(\hat{\rho})$, and the blue short dashed line means the quantum correlation $C(\hat{X}_a, \hat{\sigma}_x)$.

realistic dissipation rate of this squeezed phonon mode will be inevitably amplified without any additional cooling design. To engineer this pair of NV and MW photon into the relevant nonclassical state, we are confident that the fast dissipation route is a more suitable choice in this scheme.

Starting from the initial separated state of this whole system $|\Psi(0)\rangle_W = |0\rangle_{\text{MW}} \otimes |0\rangle_m \otimes |g\rangle_s$, since this mechanical mode possesses a large damping rate caused by MPA, its steady state will be obviously damped to the vacuum phonon state. The rest freedom with respect to the NV spin and MW photon will also be engineered into a steady state with the quantum correlation [60]. To illustrate this physical process more intuitively and clearly, we need to carry out the relevant numerical simulation on this dynamical evolution, which is dominated by the master equation $d\hat{\rho}/dt = i[\hat{\rho}, \hat{H}_{\text{ii}}^{(1)}] + \kappa_1 \mathcal{D}[\hat{a}]\hat{\rho} + \kappa_{\text{eff}}^S \mathcal{D}[\hat{b}]\hat{\rho} + \gamma \mathcal{D}[\hat{\sigma}_z]\hat{\rho}$. By setting the parameters as $\lambda = -0.7g$, $r = 2$, $\kappa_1 \sim \gamma \sim 0.01g$, and $\kappa_{\text{eff}}^S \sim 200g$, we plot the corresponding simulation results in figure 3 through solving this master equation numerically. Therein, we use three different variables to characterize this nonclassical correlation between the NV spin and MW photon: the joint variance $V(\hat{X}_a, \hat{\sigma}_x)$ with $V(\hat{X}_a, \hat{\sigma}_x) \equiv [\langle \hat{X}_a - \hat{\sigma}_x \rangle^2 - \langle \hat{X}_a \rangle \langle \hat{\sigma}_x \rangle] / 2$ and $\hat{X}_a = \hat{a} + \hat{a}^\dagger$ [62, 63], the Von Neumann entropy (VNE) with $S(\hat{\rho}) \equiv -\text{Tr}(\hat{\rho} \log_2 \hat{\rho})$ and the reduced density matrices for a subsystem of the NV spin and MW photon $\hat{\rho} = \text{Tr}_{\text{phonon}}[\hat{\rho}(t)]$ [64, 65], and the traditional quantum correlation function defined as $C(\hat{X}_a, \hat{\sigma}_x) \equiv [\langle \hat{X}_a \cdot \hat{\sigma}_x \rangle - \langle \hat{X}_a \rangle \langle \hat{\sigma}_x \rangle] / 2$ [61, 66].

The results in figure 3 clearly show that, for a given squeezing parameter $r = 2$, we can achieve an entangled steady state of this pair of NV spin and MW photon as the whole system is dynamically evolved to the moment of $\sim 10/g$. We also note that this steady state is not the

maximum entanglement, and all three different characterizations are highly consistent with our analysis above. Therefore, although there is no direct strong interaction between this pair of NV spin and MW cavity, they will be fast-engineered into a steady quantum correlated state with the assistance of this strongly damped MR. This type of application may also provide another efficient route toward the manipulation of a single NV spin with an MW photon at the single-quantum level.

5. Experimental estimations

To examine the feasibility of our scheme in realistic conditions, we now discuss the relevant experimental parameters. We consider a silicon cantilever with dimensions ($l = 11$, $w = 0.05$, $t = 0.04$) μm ; the fundamental frequency and the zero-field fluctuation can be expressed as $\omega_m \sim 3.516 \times (t/l^2) \sqrt{E/12\rho} \sim 2\pi \times 2.5$ MHz and $a_0 = \sqrt{\hbar/2m\omega_m} \sim 5.0 \times 10^{-13}$ m, respectively [67–73], the quality factor of this mechanical mode is estimated as about $Q_m \in [10^3, 10^6]$ with Young's modulus $E \sim 1.3 \times 10^{11}$ Pa, the mass density $\rho \sim 2.33 \times 10^3 \text{ kg/m}^3$, and the effective mass of this magnet-attached cantilever resonator is estimated as $m \sim 1.4 \times 10^{-17}$ kg [72, 74, 75]. With the rapid development of advanced nanotechnology, the first-order gradient magnetic field caused by the nanomagnet is expected to reach near $G_m \sim 10^6$ T/m, and we can also obtain that the magnetic coupling strength between the MR and NV spin satisfies $g \in 2\pi \times [1, 100]$ kHz [74, 76, 77]. On the other side, the fundamental frequency of this MW cavity with quality more than 10^7 is also estimated as $\omega_c \in 2\pi \times [1, 20]$ GHz [3, 4, 18, 19].

6. Conclusion

Addressing a key scientific challenge with respect to realizing direct manipulation of an NV spin at the single-quantum level with an MW cavity, we propose a hybrid system with spin–phonon–photon triple interactions, mediated by a squeezed quantum harmonic resonator. Applying the general MPA to this in-between phonon mode, we can exponentially enhance both direct spin–phonon and photon–phonon couplings, which can even further improve the coherent manipulation of an NV spin and MW photons with higher efficiency. In view of this three-body system with enhanced couplings and adjustable sidebands, this scheme may provide a more efficient phonon-mediated platform to bridge or manipulate the MW quanta and a single electron spin coherently. We also hope it can evoke wider applications in the areas of quantum state transfer and preparation, ultrasensitive detection, QND, etc. We stress that this proposed scheme is general and can be applied to others electron spins [78], such as silicon- [79, 80], germanium- [81], and tin-vacancy centers [82], and its original magnetic spin–phonon coupling mechanism can also be

applied in other devices with strain coupling or electric coupling [46–48, 50, 83, 84].

Acknowledgments

Y. Z. is supported by the National Natural Science Foundation of China under Grants No. 11 774 285, No. 11 774 282, and No. 11 504 102, the Natural Science Foundation of Hubei Province under Grants No. 2020CFB748, and No. 2019CFB788, the Research Project of Hubei Education Department under Grants No. D20201803, No. B2020079, and No. B2020078, the Doctoral Scientific Research Foundation of Hubei University of Automotive Technology (HUAT) under Grants No. BK201906, and No. BK202008, and the Foundation of Discipline Innovation Team of HUAT. H. T. R. is supported by the the Doctoral Scientific Research Foundation of Liaocheng University under Grant No. 318 052 054. Parts of the simulations are coded in PYTHON using the QUTIP library [64, 65].

Appendix A. Realizing the second-order nonlinear interaction of this MR

The main mechanism and physical image of this proposal is illustrated in figures 1(a) and (b). Working as an in-middle mediator, the Hamiltonian of this MR with a time-dependent spring constant is described as

$$H_{\text{mr}} = \frac{\hat{p}_z^2}{2m} + \frac{1}{2}k_0\hat{z}^2 + \frac{1}{2}k_\chi(t)\hat{z}^2, \quad (\text{A1})$$

where \hat{z} and \hat{p}_z are the displacement and momentum operators in the z direction, m means the effective mass of this MR, and $k_0 = \omega_m^2 m$ and $k_\chi(t) = \Delta k \cos 2\omega_\chi t$ correspond to the unperturbed fundamental spring constant (the fundamental frequency ω_m) and the time-varying spring constant, respectively. We also state that Δk is the variation of the spring constant. Applying the definition of the displacement operator $\hat{z} = z_{\text{zf}}(\hat{b}^\dagger + \hat{b})$ and the zero-field quantum fluctuation $z_{\text{zf}} = \sqrt{\hbar/2m\omega_m}$, we can quantize the MR's Hamiltonian \hat{H}_{mr} as ($\hbar = 1$),

$$\hat{H}_{\text{mr}} = \omega_m \hat{b}^\dagger \hat{b} - \Omega_\chi \cos(2\omega_\chi t)(\hat{b}^\dagger + \hat{b})^2, \quad (\text{A2})$$

where $\Omega_\chi = -\Delta k z_{\text{zf}}^2/2$ is the second-order nonlinear drive amplitude.

Appendix B. Magnetic coupling of the MR to an NV center in the dressed-state basis

For the second spin–phonon coupling part, this vibrating magnet tip produces the time-dependent gradient magnetic field $\mathbf{B}_g(t) = \mathbf{B}_g \cos \omega_m t$ and then acts on the NV spin magnetically, with the gradient magnetic field vector components $\mathbf{B}_g = (B_x, B_y, B_z)$, and the MR fundamental frequency ω_m .

Here, we note ω_m (\sim MHz) is much smaller than the NV ground-state transition frequency ($D \pm \delta/2 \sim$ GHz); these far-off resonant interactions between the NV spin and the gradient magnetic fields along the x and y directions are negligible. In the rotating frame at the frequency ω_m , the Hamiltonian for describing the magnetic interaction between the mechanical mode and the single NV center is

$$\hat{H}_{\text{sp}} = \mu_B g_e G_m \hat{z} \hat{S}_z = \lambda_0 (\hat{b}^\dagger + \hat{b}) \hat{S}_z, \quad (\text{B1})$$

where $\lambda_0 = \mu_B g_e G_m z_{\text{zf}}$ is the magnetic coupling strength with the Bohr magneton $\mu_B = 14$ GHz/T, the NV Landé factor $g_e \simeq 2$, and the first-order magnetic field gradient $G_m = \partial B_z / \partial z$. As illustrated in figure 1(c), in the bare-state basis, we can not achieve the effective spin–phonon transition interaction because of $\omega_m \ll D \pm \delta/2$, but we can utilize the dressed-state method to resolve this problem.

As shown in figure 1, to achieve the effective quantum transition interaction between the MR and the NV spin, we apply the dichromatic MW classical fields $B_x^\pm(t)$ (with frequencies ω_+ and ω_- and polarized in the x direction) to dress the state transitions $|0\rangle \leftrightarrow |\pm 1\rangle$. The Hamiltonian for describing the single NV center dressed by the dichromatic MW fields is expressed as $\hat{H}_{\text{NV}} = D \hat{S}_z^2 + \delta \hat{S}_z / 2 + \mu_B g_e [B_x^+(t) + B_x^-(t)] \hat{S}_x$, with the classical periodic driving fields $B_x^\pm(t) = B_{0x}^\pm \cos(\omega_\pm t + \phi_\pm)$. Then, we can rewrite its Hamiltonian under the rotation frame with the MW frequencies of ω_\pm ,

$$\hat{H}_{\text{NV}} = \sum_{j=\pm} -\Delta_j |j\rangle \langle j| + \frac{\Omega_j}{2} (|0\rangle \langle j| + |j\rangle \langle 0|), \quad (\text{B2})$$

where $\Delta_\pm \equiv |D - \omega_\pm \pm \delta/2|$ and $\Omega_\pm \equiv g_e \mu_B B_{0x}^\pm / \sqrt{2}$. For simplicity, we set $\Delta_\pm = \Delta$ and $\Omega_\pm = \Omega$ in the following discussions. The Hamiltonian (A1) couples the state $|0\rangle$ to a ‘bright’ state $|b\rangle = (|+1\rangle + |-1\rangle) / \sqrt{2}$, while the ‘dark’ state $|d\rangle = (|+1\rangle - |-1\rangle) / \sqrt{2}$ is decoupled. The resulting eigen basis of \hat{H}_{NV} is therefore given by $|d\rangle$ and the two dressed states $|g\rangle = \cos \theta |0\rangle - \sin \theta |b\rangle$ and $|e\rangle = \cos \theta |b\rangle + \sin \theta |0\rangle$, with the definition $\tan(2\theta) = -\sqrt{2}\Omega/\Delta$. In this dressed basis, we acquire the eigenfrequencies: $\omega_d = -\Delta$, and $\omega_{e/g} = (-\Delta \pm \sqrt{\Delta^2 + 2\Omega^2}) / \sqrt{2}$. The energy-level diagram of the bare states and the dressed states are both illustrated in figure 1(c). With the purpose of building a efficient spin–phonon transition passage, we stress that its parameters Ω and Δ are tunable here, and then we can obtain the available energy levels to match the frequency ω_m of this MR. Therefore, under the rotating wave approximation, we can rewrite the spin–phonon Hamiltonian from equations (B1)–(B2):

$$\hat{H}_{\text{sp}}^d = \sum_{r=e,d} \omega_r \hat{\sigma}_{rr} + \lambda_d \hat{b}^\dagger \hat{\sigma}_{dg}^- + \lambda_e \hat{b}^\dagger \hat{\sigma}_{ed}^- + \text{h.c.}, \quad (\text{B3})$$

where the parameters are expressed as $\omega_e \equiv \omega_e - \omega_g$, $\omega_d \equiv \omega_d - \omega_g$, $\hat{\sigma}_{ee} \equiv |e\rangle \langle e|$, $\hat{\sigma}_{dd} \equiv |d\rangle \langle d|$, $\hat{\sigma}_{gg} \equiv |g\rangle \langle g|$, $\hat{\sigma}_{dg}^- \equiv |g\rangle \langle d|$, $\hat{\sigma}_{ed}^- \equiv |d\rangle \langle e|$, $\lambda_d = -\lambda_0 \sin \theta$, and $\lambda_e = \lambda_0 \cos \theta$.

ORCID iDs

Yuan Zhou  <https://orcid.org/0000-0003-3356-1800>

References

- [1] Georgescu I M, Ashhab S and Nori Franco 2014 Quantum simulation *Rev. Mod. Phys.* **86** 153–85
- [2] Xiang Z-L, Ashhab S, You J Q and Nori F 2013 Hybrid quantum circuits: Superconducting circuits interacting with other quantum systems *Rev. Mod. Phys.* **85** 623–53
- [3] Carusotto I, Houck A A, Kollár A J, Roushan P, Schuster D I and Simon J 1919 Photonic materials in circuit quantum electrodynamics *Nat. Phys.* **16** 268–79
- [4] Blais A, Girvin S M and Oliver W D 1919 Quantum information processing and quantum optics with circuit quantum electrodynamics *Nat. Phys.* **16** 247–56
- [5] Ladd T D, Jelezko F, Laflamme R, Nakamura Y, Monroe C and O'Brien J L 2010 Quantum computers *Nature* **464** 45
- [6] Ren W *et al* 1919 Simultaneous excitation of two noninteracting atoms with time-frequency correlated photon pairs in a superconducting circuit *Phys. Rev. Lett.* **125** 133601
- [7] Liu Y-X, You J Q, Wei L F, Sun C P and Nori F 2005 Optical selection rules and phase-dependent adiabatic state control in a superconducting quantum circuit *Phys. Rev. Lett.* **95** 087001
- [8] Buluta I, Ashhab S and Nori F 2011 Natural and artificial atoms for quantum computation *Rep. Prog. Phys.* **74** 104401
- [9] Lecocq F, Ranzani L, Peterson G A, Cicak K, Jin X Y, Simmonds R W, Teufel J D and Aumentado J 2021 Efficient qubit measurement with a nonreciprocal microwave amplifier *Phys. Rev. Lett.* **126** 020502
- [10] Li P-B, Liu Y-C, Gao S-Y, Xiang Z-L, Rabl P, Xiao Y-F and Li F-L 2015 Hybrid quantum device based on NV centers in diamond nanomechanical resonators plus superconducting waveguide cavities *Phys. Rev. Appl.* **4** 044003
- [11] Romero G, García-Ripoll J J and Solano E 2009 Microwave photon detector in circuit QED *Phys. Rev. Lett.* **102** 173602
- [12] Song G-Z, Kwek L-C, Deng F-G and Long G-L 2019 Microwave transmission through an artificial atomic chain coupled to a superconducting photonic crystal *Phys. Rev. A* **99** 043830
- [13] Song C *et al* 2017 10-qubit entanglement and parallel logic operations with a superconducting circuit *Phys. Rev. Lett.* **119** 180511
- [14] Li X *et al* 2018 Perfect quantum state transfer in a superconducting qubit chain with parametrically tunable couplings *Phys. Rev. Appl.* **10** 054009
- [15] Clerk A A, Devoret M H, Girvin S M, Florian Marquardt and Schoelkopf R J 2010 Introduction to quantum noise, measurement, and amplification *Rev. Mod. Phys.* **82** 1155–208
- [16] Degen C L, Reinhard F and Cappellaro P 2017 Quantum sensing *Rev. Mod. Phys.* **89** 035002
- [17] Forn-Díaz P, Lamata L, Rico E, Kono J and Solano E 2019 Ultrastrong coupling regimes of light–matter interaction *Rev. Mod. Phys.* **91** 025005
- [18] Clerk A A, Lehnert K W, Bertet P, Petta J R and Nakamura Y 2020 Hybrid quantum systems with circuit quantum electrodynamics *Nat. Phys.* **16** 257–67
- [19] Haroche S, Brune M and Raimond J M 2020 From cavity to circuit quantum electrodynamics *Nat. Phys.* **16** 243–6
- [20] Doherty M W, Manson N B, Delaney P, Jelezko F, Wrachtrup J and Hollenberg L C L 2013 The nitrogen-vacancy colour centre in diamond *Phys. Rep.* **528** 1–45
- [21] Cai J, Retzker A, Jelezko F and Plenio M B 2013 A large-scale quantum simulator on a diamond surface at room temperature *Nat. Phys.* **9** 168
- [22] Casola F, van der Sar T and Yacoby A 2018 Probing condensed matter physics with magnetometry based on nitrogen-vacancy centres in diamond *Nat. Rev. Mater.* **3** 17088
- [23] Guo H *et al* 1919 NV center pumped and enhanced by nanowire ring resonator laser to integrate a 10 μ m-scale spin-based sensor structure *Nanotechnology* **32** 055502
- [24] Jin L, Pfender M, Aslam N, Neumann P, Yang S, Wrachtrup J and Liu R-B 2015 Proposal for a room-temperature diamond maser *Nat. Commun.* **6** 8251
- [25] Breeze J D, Salvadori E, Sathian J, Alford N M and Kay C W M 2018 Continuous-wave room-temperature diamond maser *Nature* **555** 493–6
- [26] Zhu X *et al* 2011 Coherent coupling of a superconducting flux qubit to an electron spin ensemble in diamond *Nature* **478** 221
- [27] Kubo Y *et al* 2011 Hybrid quantum circuit with a superconducting qubit coupled to a spin ensemble *Phys. Rev. Lett.* **107** 220501
- [28] Kubo Y *et al* 2010 Strong coupling of a spin ensemble to a superconducting resonator *Phys. Rev. Lett.* **105** 140502
- [29] Li P-B, Zhou Y, Gao W-B and Nori F 1919 Enhancing spin–phonon and spin–spin interactions using linear resources in a hybrid quantum system *Phys. Rev. Lett.* **125** 153602
- [30] Rabl P, Cappellaro P, Gurudev Dutt M V, Jiang L, Maze J R and Lukin M D 2009 Strong magnetic coupling between an electronic spin qubit and a mechanical resonator *Phys. Rev. B* **79** 041302
- [31] Li P-B, Xiang Z-L, Rabl P and Nori F 2016a Hybrid quantum device with nitrogen-vacancy centers in diamond coupled to carbon nanotubes *Phys. Rev. Lett.* **117** 015502
- [32] Li P-B, Li H-R and Li F-L 2016b Enhanced electromechanical coupling of a nanomechanical resonator to coupled superconducting cavities *Sci. Rep.* **6** 19065
- [33] Lü X-Y, Wu Y, Johansson J R, Jing H, Zhang J and Nori F 2015 Squeezed optomechanics with phase-matched amplification and dissipation *Phys. Rev. Lett.* **114** 093602
- [34] Nation P D, Johansson J R, Blencowe M P and Nori F 2012 Colloquium: Stimulating uncertainty: Amplifying the quantum vacuum with superconducting circuits *Rev. Mod. Phys.* **84** 1–24
- [35] Muñoz C S, Lara A, Puebla J and Nori F 2018 Hybrid systems for the generation of nonclassical mechanical states via quadratic interactions *Phys. Rev. Lett.* **121** 123604
- [36] Qin W, Miranowicz A, Li P-B, Lü X-Y, You J Q and Nori F 2018 Exponentially enhanced light–matter interaction, cooperativities, and steady-state entanglement using parametric amplification *Phys. Rev. Lett.* **120** 093601
- [37] Leroux C, Govia L C G and Clerk A A 2018 Enhancing cavity quantum electrodynamics via antisqueezing: synthetic ultrastrong coupling *Phys. Rev. Lett.* **120** 093602
- [38] Lemonde M-A, Didier N and Clerk A A 2016 Enhanced nonlinear interactions in quantum optomechanics via mechanical amplification *Nat. Commun.* **7** 11338
- [39] Blum S, O'Brien C, Lauk N, Bushev P, Fleischhauer M and Morigi G 2015 Interfacing microwave qubits and optical photons via spin ensembles *Phys. Rev. A* **91** 033834
- [40] Li B, Li P-B, Zhou Y, Ma S-L and Li F-L 2017 Quantum microwave–optical interface with nitrogen-vacancy centers in diamond *Phys. Rev. A* **96** 032342
- [41] Taylor J M, Cappellaro P, Childress L, Jiang L, Budker D, Hemmer P R, Yacoby A, Walsworth R and Lukin M D 2008

- High-sensitivity diamond magnetometer with nanoscale resolution *Nat. Phys.* **4** 810–6
- [42] Tang Y-C, Li Y-S, Hao L, Hou S-Y and Long G L 2012 Quantum-nondemolition determination of an unknown Werner state *Phys. Rev. A* **85** 022329
- [43] Szorkovszky A, Clerk A A, Doherty A C and Bowen W P 2014 Mechanical entanglement via detuned parametric amplification *New J. Phys.* **16** 063043
- [44] Szorkovszky A, Doherty A C, Harris G I and Bowen W P 2011 Mechanical squeezing via parametric amplification and weak measurement *Phys. Rev. Lett.* **107** 213603
- [45] Rugar D and Grütter P 1991 Mechanical parametric amplification and thermomechanical noise squeezing *Phys. Rev. Lett.* **67** 699
- [46] Teissier J, Barfuss A, Appel P, Neu E and Maletinsky P 2014 Strain coupling of a nitrogen-vacancy center spin to a diamond mechanical oscillator *Phys. Rev. Lett.* **113** 020503
- [47] Meesala S, Sohn Y-I, Atikian H A, Kim S, Burek M J, Choy J T and Lončar M 2016 Enhanced strain coupling of nitrogen-vacancy spins to nanoscale diamond cantilevers *Phys. Rev. Appl.* **5** 034010
- [48] MacQuarrie E R, Otten M, Gray S K and Fuchs G D 2017 Cooling a mechanical resonator with nitrogen-vacancy centres using a room temperature excited state spin-strain interaction *Nat. Commun.* **8** 14358
- [49] Cai J, Jelezko F and Plenio M B 2014 Hybrid sensors based on colour centres in diamond and piezoelectric layers *Nat. Commun.* **5** 4065
- [50] Ovarthaiyapong P, Lee K W, Myers B A and Jayich A C B 2014 Dynamic strain-mediated coupling of a single diamond spin to a mechanical resonator *Nat. Commun.* **5** 4429
- [51] Aspelmeyer M, Kippenberg T J and Marquardt F 2014 Cavity optomechanics *Rev. Mod. Phys.* **86** 1391
- [52] Kronwald A, Marquardt F and Clerk A A 2013 Arbitrarily large steady-state bosonic squeezing via dissipation *Phys. Rev. A* **88** 063833
- [53] Kienzler D, Lo H-Y, Keitch B, de Clercq L, Leupold F, Lindenfeller F, Marinelli M, Negnevitsky V and Home J P 2015 Quantum harmonic oscillator state synthesis by reservoir engineering *Science* **347** 53
- [54] Wollman E E, Lei C U, Weinstein A J, Suh J, Kronwald A, Marquardt F, Clerk A A and Schwab K C 2015 Quantum squeezing of motion in a mechanical resonator *Science* **349** 952
- [55] Pirkkalainen J-M, Damskägg E, Brandt M, Massel F and Sillanpää M A 2015 Squeezing of quantum noise of motion in a micromechanical resonator *Phys. Rev. Lett.* **115** 243601
- [56] Cirac J I, Parkins A S, Blatt R and Zoller P 1993 Dark squeezed states of the motion of a trapped ion *Phys. Rev. Lett.* **70** 556
- [57] Ma S-L, Li X-K, Liu X-Y, Xie J-K and Li F-L 2019 Stabilizing Bell states of two separated superconducting qubits via quantum reservoir engineering *Phys. Rev. A* **99** 042336
- [58] Lü D-Y, Wang G H, Zhou Y, Xu L and Wang Q L 2021 Collective decay induce quantum phase transition in a well-controlled hybrid quantum system *Results Phys.* **21** 103832
- [59] Zhou Y, Li B, Li X-X, Li F-L and Li P-B 2018 Preparing multiparticle entangled states of nitrogen-vacancy centers via adiabatic ground-state transitions *Phys. Rev. A* **98** 052346
- [60] Li P 2008 Generation of two-mode field squeezing through selective dynamics in cavity QED *Phys. Rev. A* **77** 015809
- [61] Zhou T, Cui J and Long G L 2011 Measure of nonclassical correlation in coherence-vector representation *Phys. Rev. A* **84** 062105
- [62] Ma S-L, Li Z, Fang A-P, Li P-B, Gao S-Y and Li F-L 2014 Controllable generation of two-mode-entangled states in two-resonator circuit QED with a single gap-tunable superconducting qubit *Phys. Rev. A* **90** 062342
- [63] Li P-B, Gao S-Y and Li F-L 2012 Engineering two-mode entangled states between two superconducting resonators by dissipation *Phys. Rev. A* **86** 012318
- [64] Johansson J R, Nation P D and Nori F 2012 Qutip: An open-source Python framework for the dynamics of open quantum systems *Comput. Phys. Commun.* **183** 1760–72
- [65] Johansson J R, Nation P D and Nori F 2013 Qutip 2: A Python framework for the dynamics of open quantum systems *Comput. Phys. Commun.* **184** 1234–40
- [66] Zeng B, Chen X, Zhou D-L and Wen X-G 2015 Quantum information meets quantum matter—from quantum entanglement to topological phase in many-body systems arXiv:1508.02595
- [67] Sidles J A, Garbini J L, Bruland K J, Rugar D, Züger O, Hoen S and Yannoni C S 1995 Magnetic resonance force microscopy *Rev. Mod. Phys.* **67** 249–65
- [68] Imboden M and Mohanty P 2014 Dissipation in nanoelectromechanical systems *Phys. Rep.* **534** 89–146
- [69] Atatüre M, Englund D, Vamivakas N, Lee S-Y and Wrachtrup J 2018 Scalable architecture for a room temperature solid-state quantum information processor *Nat. Rev. Mater.* **3** 38
- [70] Li M, Tang H X and Roukes M L 2007 Ultra-sensitive NEMS-based cantilevers for sensing, scanned probe and very high-frequency applications *Nat. Nanotechnol.* **2** 114
- [71] Ekinci K L and Roukes M L 2005 Nanoelectromechanical systems *Rev. Sci. Instrum.* **76** 061101
- [72] Yang J, Ono T and Esashi M 2000 Surface effects and high quality factors in ultrathin single-crystal silicon cantilevers *Appl. Phys. Lett.* **77** 3860–2
- [73] Brantley W A 1973 Calculated elastic constants for stress problems associated with semiconductor devices *J. Appl. Phys.* **44** 534–5
- [74] Tao Y, Eichler A, Holzherr T and Degen C L 2016 Ultrasensitive mechanical detection of magnetic moment using a commercial disk drive write head *Nat. Commun.* **7** 12714
- [75] Tao Y, Boss J M, Moores B A and Degen C L 2014 Single-crystal diamond nanomechanical resonators with quality factors exceeding one million *Nat. Commun.* **5** 3638
- [76] Meyer E and Rast S 2007 Magnetic tips probe the nanoworld *Nat. Nanotechnol.* **2** 267–8
- [77] Mamin H J, Poggio M, Degen C L and Rugar D 2007 Nuclear magnetic resonance imaging with 90-nm resolution *Nat. Nanotechnol.* **2** 301–6
- [78] Thiering G and Gali A 2018 Ab initio magneto-optical spectrum of group-IV vacancy color centers in diamond *Phys. Rev. X* **8** 021063
- [79] Hepp C et al 2014 Electronic structure of the silicon vacancy color center in diamond *Phys. Rev. Lett.* **112** 036405
- [80] Sipahigil A, Jahnke K D, Rogers L J, Teraji T, Isoya J, Zibrov A S, Jelezko F and Lukin M D 2014 Indistinguishable photons from separated silicon-vacancy centers in diamond *Phys. Rev. Lett.* **113** 113602
- [81] Bhaskar M K et al 2017 Quantum nonlinear optics with a germanium-vacancy color center in a nanoscale diamond waveguide *Phys. Rev. Lett.* **118** 223603
- [82] Iwasaki T, Miyamoto Y, Taniguchi T, Siyushev P, Metsch M H, Jelezko F and Hatano M 2017 Tin-vacancy quantum emitters in diamond *Phys. Rev. Lett.* **119** 253601
- [83] Rabl P, Kolkowitz S J, Koppens F H L, Harris J G E, Zoller P and Lukin M D 2010 A quantum spin transducer based on nanoelectromechanical resonator arrays *Nat. Phys.* **6** 602–8
- [84] Dolde F, Fedder H, Doherty M W, Nöbauer T, Rempp F, Balasubramanian G, Wolf T, Reinhard F, Hollenberg L C L and Jelezko F 2011 Electric-field sensing using single diamond spins *Nat. Phys.* **7** 459–63